

## NEAR-INFRARED AND ULTRAVIOLET SPECTROPHOTOMETRY OF SYMBIOTIC NOVAE

RICHARD J. RUDY,<sup>1</sup> STEVEN R. MEIER,<sup>1,2</sup> GEORGE S. ROSSANO,<sup>1</sup> DAVID K. LYNCH,<sup>1</sup>  
R. C. PUETTER,<sup>1,3</sup> AND PETER ERWIN<sup>1,4</sup>

Received 1998 March 26; accepted 1998 November 11

### ABSTRACT

In this paper we present an atlas of near-infrared spectrophotometry of symbiotic novae and report results from nearly contemporaneous *IUE* observations. The data cover RT Ser, AG Peg, V1016 Cyg, V1329 Cyg, HM Sge, and Pu Vul, most of the known symbiotic novae that are observable from the northern hemisphere. Emission-line strengths for both spectral regions are tabulated. Extinction values are derived from He II  $\lambda 1640$  in the UV and He II  $\lambda 10124$  in the infrared. Spectral types are determined for the cool giant component using infrared absorption features. The extinction and apparent  $J$  ( $1.25 \mu\text{m}$ ) magnitude measured from the spectrophotometry are combined with the known relation between spectral type and absolute magnitude to derive distances for each system.

*Subject headings:* binaries: symbiotic — infrared: stars — novae, cataclysmic variables

### 1. INTRODUCTION

Symbiotic novae represent a subclass of symbiotic stars that undergo a single, or very infrequent, nova-like outburst (Viotti 1988). This subclass originally contained only seven objects: AG Peg, RT Ser, RR Tel, V1016 Cyg, V1329 Cyg (=HBV 475), HM Sge, and AS 239 (=V2110 Oph) (Allen 1980a). PU Vul was identified later, and recent studies (Bragaglia et al. 1995; Ivison & Seaquist 1995) have added three additional members, while the classification of V2110 Oph has been questioned (Murset & Nussbaumer 1994, hereafter MN). Symbiotic novae differ from classical novae in several respects: (1) In symbiotic novae the companion star is a late-type giant rather than a dwarf. This results in much smaller outburst amplitudes since the preoutburst optical and infrared brightness is determined by the giant. However, the total energy associated with the outburst of a symbiotic nova may significantly exceed that of a classical nova. (2) Symbiotic systems are widely separated rather than close binaries, with orbital periods that vary from two to several dozen years, instead of a few days. As such, the emission-line region that results from the transfer of mass from the late-type star to the hot companion arises from a stellar wind rather than Roche lobe overflow. Moreover, the emission-line region does not envelope both stars, even during outburst. (3) The increase to maximum brightness usually takes several months, not the few days characteristic of classical novae. (4) Similarly, the return to preoutburst brightness is also much slower, with emission lines persisting for decades instead of months or years.

Because the emission-line regions associated with the outburst of a symbiotic nova evolve over such long periods, it is important to provide a series of observations that mon-

itors this evolution. Largely because of the *International Ultraviolet Explorer* satellite (*IUE*), numerous measurements exist that allow one to follow the UV spectral development (Meier et al. 1994, and references therein), but the number of corresponding infrared studies is sparse. In this paper we present infrared spectrophotometry in the wavelength region  $0.9\text{--}1.3 \mu\text{m}$  for many of the known symbiotic novae. These data provide a base epoch to which later observations of the rich infrared emission-line spectra may be compared. In addition, the near-infrared is the optimum region in which to study the giant since it includes the peak emission from the giant, and contamination by the hot component, and thermal dust emission, which dominate in the ultraviolet and thermal infrared, respectively, are very small. From our observations, spectral types are determined for the cool component in each system.

To expand on the results derivable from our infrared spectrophotometry, we present nearly concurrent UV spectra and emission-line strengths. From this combined database, He II lines at  $1640 \text{ \AA}$  and  $10124 \text{ \AA}$  are used to measure the extinction. The extinction values are used to correct the apparent  $J$ -band magnitudes for reddening; the latter are then compared to the absolute  $J$  magnitudes derived from the spectral types of the giant components to determine distances for each system.

### 2. OBSERVATIONS

Journals of the infrared and ultraviolet observations are presented in Tables 1 and 2, respectively. All infrared data were obtained using the Aerospace near-infrared spectrometer with the 3 m Shane telescope of Lick Observatory. The spectrometer scanned a  $600 \text{ line mm}^{-1}$  grating, providing a spectral resolution that varies from  $\lambda/\Delta\lambda \sim 350$  at  $0.95 \mu\text{m}$  to  $\sim 550$  at  $1.3 \mu\text{m}$ , where  $\Delta\lambda$  is the measured FWHM of an unresolved feature at the wavelength  $\lambda$ . To provide higher quality spectra, the spacing between data points was chosen to be one-quarter of a resolution element. The detector was a germanium photodiode used with a charge integrating amplifier. The aperture was oval in shape with major and minor axes of  $9''.6$  and  $8''.1$ , respectively. Sky subtraction was performed by redirecting the telescope to a patch of sky near the source.

To correct for telluric absorption, the raw spectrum of each symbiotic nova was divided by a comparison star. The

<sup>1</sup> Space and Environment Technology Center, The Aerospace Corporation, M2/266, P.O. Box 92957, Los Angeles, CA 90009; email: richard.j.rudy@aero.org, david.k.lynnch@aero.org, george.s.rossano@aero.org.

<sup>2</sup> Current address: Optical Sciences Division, Naval Research Laboratory, Code 5622, Washington, DC 20375; email: meier@ccf.nrl.navy.mil.

<sup>3</sup> Center for Astrophysics and Space Sciences, University of California, San Diego, 9500 Gilman Drive, Code 0111, La Jolla, CA 92093; email rpuetter@ucsd.edu.

<sup>4</sup> Current address: Department of Astronomy, University of Wisconsin, 475 North Charter Street Madison, WI 53706; email erwin@madraf.astro.wisc.edu.

TABLE 1  
JOURNAL OF INFRARED  
OBSERVATIONS

Object	Date
AG Peg .....	1989 Jul 14
RT Ser .....	1989 Jul 14
HM Sge .....	1988 Jul 6
	1989 Jul 13
V1016 Cyg .....	1988 Jul 6
	1989 Apr 26
V1329 Cyg .....	1989 Jul 14
PU Vul .....	1989 Jul 14

comparison stars were giants of spectral type G8 to K3, a range chosen for the absence of the Paschen series and to minimize other absorption features. The flux calibrations of the comparison stars were based on the absolute flux calibration of  $\alpha$  Lyr reported by Hayes & Latham (1975). The spectral shapes were drawn from the models of Kurucz (1991). Plots of the infrared spectra for the six symbiotic novae are presented in Figures 1, 2c, 3, 4, 5, and 6c. Emission-line identifications and intensities are given in Tables 3B–8B; errors in the absolute intensities are estimated to be  $\leq 15\%$  for the stronger features, with uncertainties in relative line strengths  $\leq 10\%$ .

The *IUE* ultraviolet spectra were obtained from the *IUE* Reduction Data Analysis Facility (IUEDAF) data archives at NASA/Goddard Space Flight Center (NASA/GSFC). With the exception of RT Ser, UV spectra were available within several months of the IR observations. A total of eight SWP ( $\lambda\lambda 1200$ – $2000$ ), seven LWP ( $\lambda\lambda 2000$ – $3200$ ), and one LWR ( $\lambda\lambda 2000$ – $3200$ ) low-resolution (LORES) ultraviolet spectra were retrieved and analyzed. The UV spectra were obtained with the  $10'' \times 20''$  large aperture *IUE* spectrometer, which has a limiting spectral resolution of 6–8 Å in low-dispersion mode. All wavelengths and absolute line intensities were calculated using the data reduction routines at the IUEDAF at NASA/GSFC. Line identifications for the less familiar emission lines in the LWP ( $\lambda\lambda 2000$ – $3200$ ) wavelength range, particularly the Fe II lines, were drawn from the identifications of the fea-

TABLE 2  
JOURNAL OF *IUE* OBSERVATIONS

Object	Camera/Image Sequence Number	Date	Exposure (minutes)
AG Peg .....	SWP 37419	1989 Oct 21	6
	LWP 16594	1989 Oct 21	6
RT Ser .....	SWP 42160	1991 Aug 2	90
	LWR 14047	1982 Aug 29	55
HM Sge .....	SWP 33154	1988 Mar 25	10
	LWP 12919	1988 Mar 25	9
	SWP 36951	1989 Sep 7	10
	LWP 16297	1989 Sep 7	10
V1016 Cyg .....	SWP 33783	1988 Jun 19	6
	LWP 13464	1988 Jun 21	25
	SWP 36824	1989 Aug 12	6
	LWP 16106	1989 Aug 12	15
V1329 Cyg .....	SWP 35973	1989 Apr 10	60
	LWP 15333	1989 Apr 10	60
PU Vul .....	SWP 37184	1989 Sep 24	16.7
	LWP 16416	1989 Sep 25	5.3

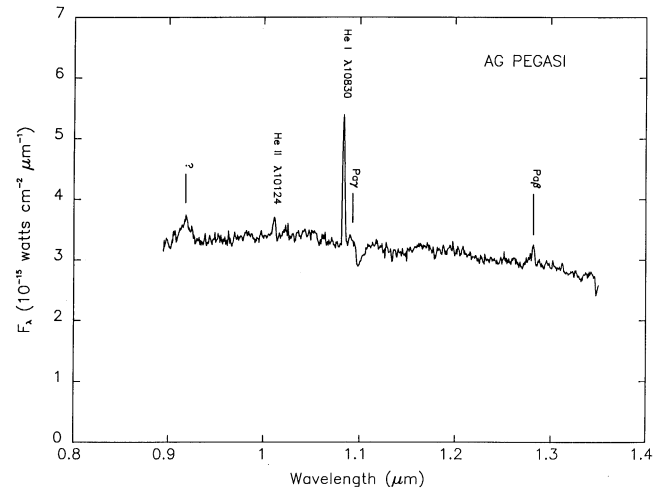


FIG. 1.—Near-infrared spectrum of AG Peg. The emission lines are characteristic of a high-density, high-excitation region with the intensity of He I  $\lambda 10830$  and He II  $\lambda 10124$  and  $\lambda 11626$  relative to Pa $\beta$  and Pa $\gamma$  suggesting an overabundance of helium. The absence of detectable forbidden lines indicates gas densities greater than  $10^6 \text{ cm}^{-3}$ . The infrared continuum is the bluest of any of the six symbiotic novae we observed; there is no trace of the infrared TiO absorptions although their optical counterparts are prominent (KF).

tures in RR Tel by Penston et al. (1983) and Doschek & Feibelman (1993). The *IUE* LORES spectra presented have been corrected for sensitivity degradation in the SWP and LWP cameras using software routines developed at the IUEDAF. The LWR spectrum of RT Ser, taken in 1982, has been reprocessed using the most current *IUE* SIPS (*IUE* Signal Image Processing System) data calibration and extraction procedures. Because of the large number of *IUE* spectra of symbiotic novae already present in the literature (e.g., Murset et al. 1991; Vogel & Nussbaumer 1992; MN; Meier et al. 1994), we show only those of RT Ser and PU Vul—RT Ser because, to our knowledge, the UV spectra have not been published previously, and PU Vul because its spectrum was still evolving at the time of our observations. These data are shown in Figures 2a, 2b and 6a and 6b; respectively. Line fluxes for all the objects are presented in Tables 3A–8A. The absolute line intensities are affected by the calibration errors and by the signal-to-noise ratio of the feature and the nearby continuum. Two of the spectra that we employed (HM Sge from 1988 March 25 and V1016 Cyg from 1988 June 19) have had fluxes for He II  $\lambda 1640$  reported previously in the literature (MSVN). In both cases the values reported by us are 6% larger, perhaps due to slight changes in the *IUE* calibration levels. Other than uncertainties in the absolute flux calibration, additional errors in the measurement of the line fluxes arise from blending with other features and placement of the continuum. Allowing for all of these, we estimate that uncertainties in the absolute line fluxes should be better than 15% for moderately strong lines and 25% for weaker ones.

As noted above, the number of near-infrared spectrophotometric studies of symbiotic novae in the literature is small. References that do present data which overlap our spectral region include Andriolat (1982): data for AG Peg, HM Sge, V1016 Cyg, V1329 Cyg; Baratta et al. (1991): AG Peg; Rudy et al. (1990): V1016 Cyg (observations which are included in this work); Schmid & Schild (1990): measurements of Pa $\delta$  and He II  $\lambda 10124$  in V1016 Cyg, HM Sge, and

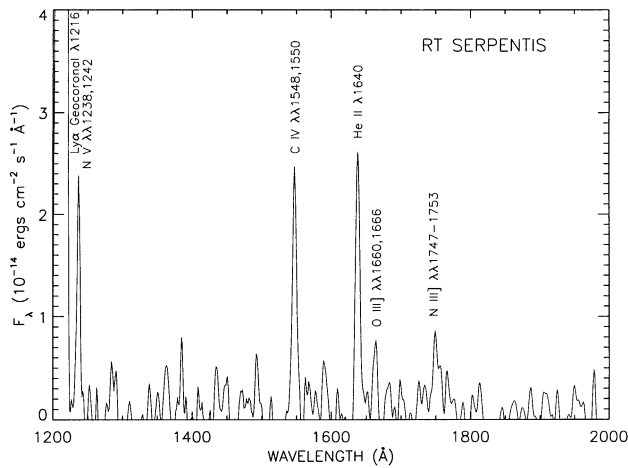


FIG. 2a

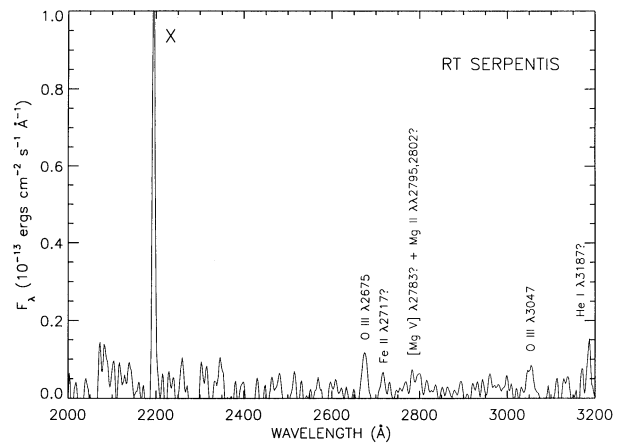


FIG. 2b

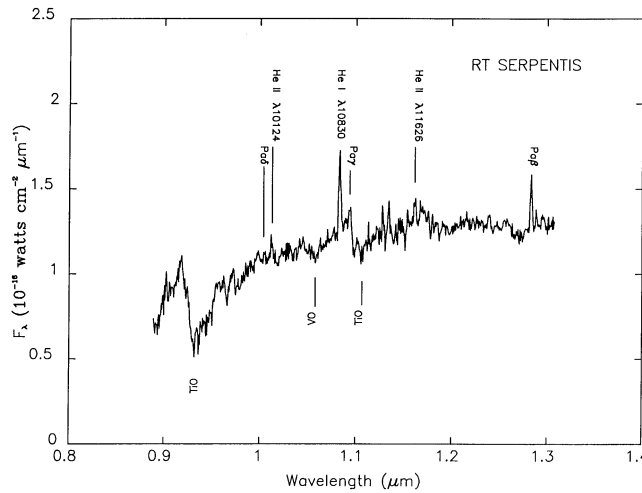


FIG. 2c

FIG. 2.—(a) SWP spectrum of RT Ser from 1991 Aug. Permitted lines of N v, C iv, and He II dominate. No continuum was detected. (b) LWR spectrum of RT Ser (from 1982 March 2). The “X” indicates a cosmic-ray hit. The spectrum is very faint, but O III  $\lambda$ 2675 and  $\lambda$ 3047 are detected. (c) Near-infrared spectrum of RT Ser (from 1989 July). The strong continuum is due to the M giant; the deep absorption at 0.93  $\mu$ m is due mainly to TiO. Together with the detectable VO trough at 1.05  $\mu$ m, this indicates a spectral type of M5.5. The emission line region, although weak, produces the Paschen series. He II features, and the strong He I  $\lambda$ 10830 characteristic of most symbiotic novae.

V1329 Cyg; Kelly & Latter (1995): V1016 Cyg; Bensammar et al. (1991); PU Vul; Fried (1990a: 1990b): RT Ser; Andriolat & Houziaux (1994): PU Vul. Pertinent near-infrared photometric studies include Allen (1982), Kenyon (1988), Munari et al. (1992), and Ananth & Leahy (1993).

3. RESULTS

The infrared spectra of this small sample of objects encompass a broad range of behavior. As gauged by their infrared emission lines, there exists a rough progression based loosely on the time since outburst, in the sense that “older” spectra display fewer and weaker infrared emission lines. Viotti (1988) gives the following approximate times of outburst: AG Peg:  $\sim$ 1855; RT Ser: 1909; HM Sge: 1975; V1016 Cyg: 1964; V1329 Cyg: 1966; PU Vul: 1978. Thus the “oldest” spectrum is that of AG Peg; at present its lines form in a matter bounded nebula (Murset et al. 1991) and its infrared features are limited to the recombination lines of H and He II and the largely collisionally excited  $\lambda$ 10830 line of He I. The second oldest, RT Ser, has a similar spectrum, but also emits O I  $\lambda$ 8446 (Fried 1990a, 1990b), a line fluores-

cently excited by Ly $\beta$  and a feature we associate with younger outbursts (see below). Objects with more recent eruptions such as HM Sge and V1016 Cyg have the same H and He features at greater equivalent widths than the older symbiotic novae, but also have extended emission-line regions with densities low enough to form prominent forbidden lines. V1016 Cyg, in addition, supports a high-density, partially neutral region in which Ly $\beta$  fluorescence excites the strong O I  $\lambda$ 1304,  $\lambda$ 8446, and  $\lambda$ 11287 features (Grandi 1980). The O I lines are even more pronounced in V1329 Cyg, where the low-excitation Ca II infrared triplet is present and densities are high enough that infrared forbidden lines are absent entirely. PU Vul forms the end of this progression. Optical depths within its emission-line region are sufficient, and excitations low enough, that numerous Fe II features appear in addition to the O I and Ca II lines. While interesting this progression is simply used to determine the order in which the objects are discussed—the discussion itself focuses on the reddening (measured from the He II lines but supplemented with results from the O I features), the classification of the giant companions, and

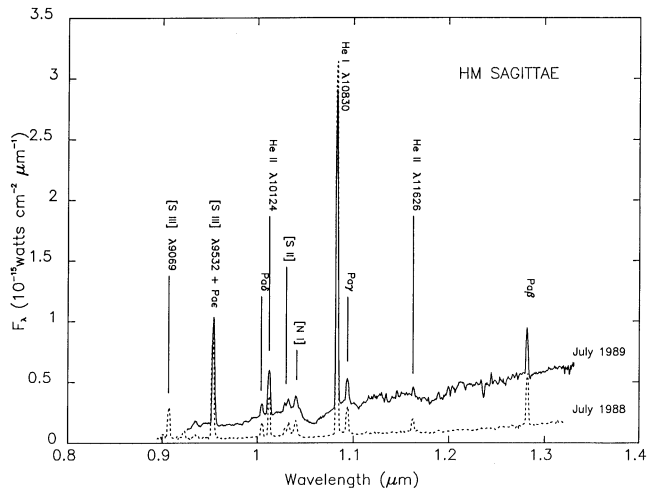


FIG. 3.—IR spectra of HM Sge taken approximately 1 yr apart. The Mira companion has a period of  $\sim 540$  days, and its variations are seen clearly in the change of the continuum, e.g., the much stronger VO absorption at  $1.05 \mu\text{m}$  at the later epoch. The increase in the near-infrared brightness with the shift to later spectral type is characteristic of mira variability. Note that despite the large variations in continuum the changes in the strengths of the emission lines are small.

the distances that are derivable using the first two parameters.

### 3.1. Reddening Estimates

With one caveat (discussed below), the He II features  $\lambda 1640$  and  $\lambda 10124$  together provide a nearly ideal reddening indicator for objects with strong He II emission. The lower abundance of helium mitigates the optical depth effects that complicate the interpretation of the hydrogen lines. The ultraviolet He II lines alone have been shown to be generally reliable for reddening measurements (Schmid & Schild 1990), and the very large wavelength interval that separates  $\lambda 1640$  from  $\lambda 10124$  provides for much greater differential

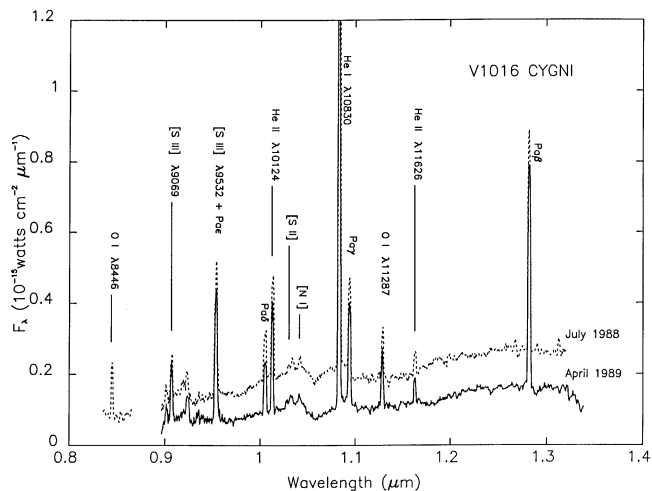


FIG. 4.—Infrared spectra of V1016 Cyg. Like the measurements of HM Sge, the continuum shows the variations of the Mira companion, which has a period of 450 days. The 1988 spectrum has been discussed in detail by Rudy et al. (1990). The presence of the strong O I lines excited by Ly $\beta$  fluorescence indicate that H $\alpha$  is optically thick in at least a portion of the emission-line region. This places V1016 Cyg intermediate between objects like HM Sge, which manifests no O I emission, and objects such as V 1329 Cyg (Fig. 5c) and PU Vul (Fig. 6c) which display Ca II and Fe II emission as well as O I.

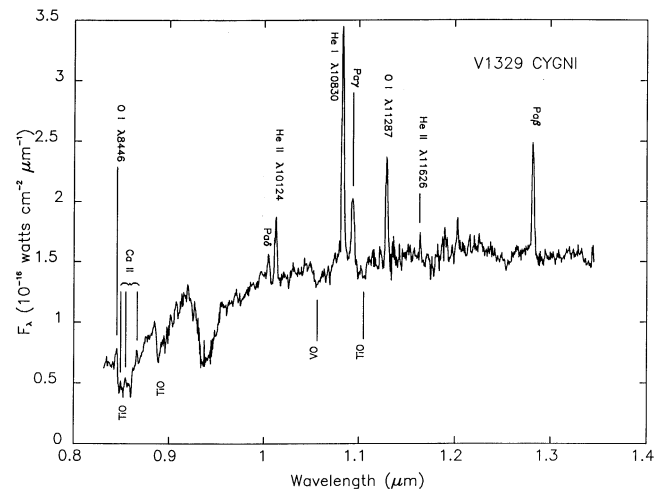


FIG. 5.—Near-infrared spectrum of V1329 Cyg. The emission lines span a broad range of ionization: the He II features are strong but O I  $\lambda 8446$  and  $\lambda 11287$  (which are excited by Ly $\beta$  fluorescence) are also prominent, and the Ca II infrared triplet is present. The latter indicates the existence of a region with greater optical depth than any present in V1016 Cyg. The absence of detectable forbidden lines, particularly [S II], [S III], and [N I] indicate densities in the emission line region significantly larger than  $10^6 \text{ cm}^{-3}$ . V1329 Cyg displays an infrared continuum which is virtually identical to that of RT Ser—for the same reasons we also classify it as spectral type M5.5.

extinction. To estimate the intrinsic line ratios we used the case B values given by Hummer & Storey (1987), and to describe the reddening, the prescription of Savage & Mathis (1979) was employed. Table 9 presents extinction values for the symbiotic novae derived in this manner; extinction values obtained in different ways and compiled by MN are included for comparison.

The caveat mentioned above arises from conditions peculiar to symbiotic stars. Depending on the line of sight of the observer, the wind from the cool giant can block flux from the emission-line region of the hot component; in extreme cases the wind will envelope the emission-line region entirely. In a process described by Shore & Aufdenberger (1993), material in the wind, particularly ions of iron, absorb strongly in the ultraviolet. The absorption of He II  $\lambda 1640$  can be especially pronounced, e.g., in the symbiotic system Z And it results in order-of-magnitude variations in the line flux as the binary moves through its orbit (Mikolajewska & Kenyon 1996). Since this mechanism does not similarly affect He II  $\lambda 10124$ , the reddening derived from its ratio to  $\lambda 1640$  would thus appear to vary with orbital phase.

To gauge the possible impact of this effect on the symbiotic novae in our sample, we examined high-resolution IUE observations, checked orbital phases at the times of our measurements, and computed reddening values in alternative ways. The results for each system follow. For RT Ser, there is only one epoch of observations, and they are of low resolution and poor quality (see Figs. 2a and 2b) so we cannot address the question of UV absorption either directly or as a possible cause of variability. PU Vul, with its eclipsing orbit and strong Fe II emission, certainly has UV absorption, but its He II emission was too weak for us to measure the reddening. For V1016 Cyg and HM Sge, Schmid & Schild (1990) did not see evidence for selective absorption of  $\lambda 1640$  in their high-resolution observations. Similarly, high-resolution observations of AG Peg (also from 1989 October 28) show no obvious absorption of

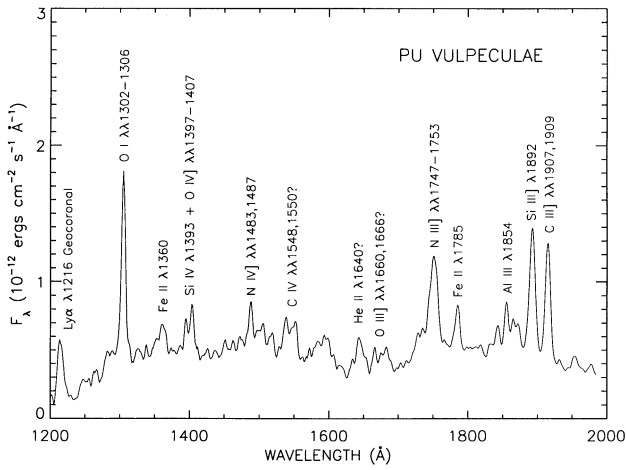


FIG. 6a

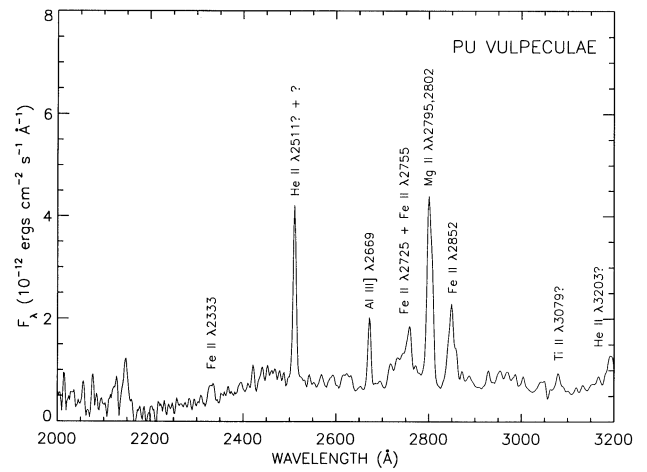


FIG. 6b

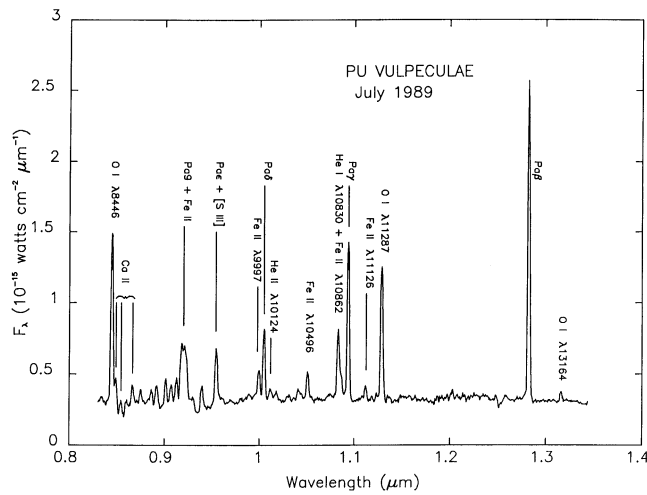


FIG. 6c

FIG. 6.—(a) Ultraviolet (SWP) spectrum of PU Vul. The Ly $\beta$  fluoresced O I lines  $\lambda\lambda$ 1302–1306 are distinct. Also present are Fe II  $\lambda$ 1360, Si IV  $\lambda$ 1393 + O IV]  $\lambda\lambda$ 1397–1407, N III]  $\lambda\lambda$ 1747–1753, Fe II  $\lambda$ 1785, Al III  $\lambda$ 1854, Si III]  $\lambda$ 1892, and C III]  $\lambda\lambda$ 1907, 1909 superposed on a strong UV continuum. (b) Ultraviolet (LWP) spectrum of PU Vul. The spectrum displays lines Al III]  $\lambda$ 2669, Fe II  $\lambda$ 2725 + Fe II  $\lambda$ 2755, Mg II  $\lambda\lambda$ 2795,2802, Fe II  $\lambda$ 2852 and possibly Ti II  $\lambda$ 3079 on an ultraviolet continuum that rises with wavelength. The 2200 Å interstellar absorption depression is clearly seen in the LWP spectrum. Given the weakness of  $\lambda$ 1640, the feature at 2511 Å is not He II  $\lambda$ 2511. (c) Infrared spectrum of PU Vul. PU Vul represents the one extreme in the range of emission lines seen in the symbiotic novae, showing no obvious forbidden lines, weak or absent He II (the feature in the vicinity of He II  $\lambda$ 10124 is probably not He II), very weak He I  $\lambda$ 10830, and low-excitation features such as the O I, Fe II, and Ca II arising from a warm, sheltered region in which a significant fraction of the hydrogen is neutral. While V1016 Cyg, V1329 Cyg, and AG Peg display O I, and V1329 Cyg shows Ca II emission, PU Vul is the only object in our data set with prominent Fe II features. All of the Fe II lines in this spectrum are believed to result from cascades fluorescently excited by Ly $\alpha$  (Johansson & Jordan 1984; Johansson 1990; Hamann et al. 1994). The Fe II lines ranging from  $\lambda$ 9997 through  $\lambda$ 11126 have been discussed by Rudy et al. (1991, 1992). The feature shown at 1.0496  $\mu$ m is a blend of Fe II  $\lambda$ 10490 and  $\lambda$ 10501. The identification of the giant component as  $\sim$ M4 is based largely on the TiO feature at 0.93  $\mu$ m.

$\lambda$ 1640. Moreover, the ephemeris for AG Peg (Slovak & Lamber 1988) indicates that the system was near quadrature at the time of our observation (phase 0.78, where the giant component is in front at phase 0.0), so the expected absorption by the wind from the giant is expected to be small.

The remaining object is V1329 Cyg, an eclipsing system with a period of 956 days. The ephemerides of Hric, Chochol, & Komzik (1993) and Schild & Schmid (1997) indicate a phase of 0.86 or 0.87, where phase 0.0 (or 1.0) corresponds to maximum obscuration of the hot component by its cool companion. Lacking high-resolution observations of  $\lambda$ 1640, we attempted to compute the reddening by substituting He II  $\lambda$ 3203 (the 5–3 transition of He<sup>+</sup>) and  $\lambda$ 2733 (6–3) for  $\lambda$ 1640. Although these features are weaker than  $\lambda$ 1640 and do not afford quite as much differ-

ential extinction, inspection of the line list of Kurucz (1988) indicates that they are comparatively free of absorption by Fe<sup>+</sup>. He II  $\lambda$ 3203 was difficult to measure in this object, but  $\lambda$ 2733, together with  $\lambda$ 10124, gives a reddening value identical to the entry in Table 9.

Besides selective absorption of  $\lambda$ 1640, the other major source of error in our values arises from potential source variability and the nonsimultaneity of the IR and UV measurements. To assess the variability in each of the symbiotic novae, we reviewed additional *IUE* measurements around the time of our observations. Again, RT Ser was not considered because only a single epoch of data exists, nor was PU Vul, since its extinction is derived from the infrared data alone. The  $\lambda$ 1640 fluxes reported from AG Peg by MNSV show a steady decline from 330 ( $\times 10^{-12}$  ergs cm<sup>-2</sup> s<sup>-1</sup>) in 1980, to 250 in 1985, to 110 in 1990. The last measurement

TABLE 3

## A. ULTRAVIOLET EMISSION-LINE STRENGTHS FOR AG PEGASI

Ion	Wavelength (Å)	$F/F(\text{He II } \lambda 1640)^a$
N v	1241.7	1.70 <sup>b</sup>
O I?	1306.1	0.035
O v	1373.3	0.097
Si IV	blended with O IV]	...
O IV]	1402.6	0.58 <sup>b</sup>
N IV]	1487.7	0.64 <sup>b</sup>
C IV	1550.3	1.42 <sup>b</sup>
[Ne v]?	1577.9	0.045
He II	1641.9	1.00 <sup>b</sup>
O III]	1666.1	0.36 <sup>b</sup>
Si II	1720.6	0.081
N III]	1752.5	0.13
Si II	1821.8	0.061
Si III]	1892.9	0.061
C III]	1910.2	0.12
He II + ?	2249.6	0.39
He II	2307.2	0.026
Fe II + He II	2385.6	0.049
[Ne IV]	2423.2	0.024
Fe II	2436.0	0.019
Fe II	2482.0	0.036
He II	2512.2	0.11 <sup>b</sup>
Fe II	2597.4	0.020
Fe II	2615.7	0.017
He II	2733.7	0.11 <sup>b</sup>
[Mg v]	2783.8	0.11 <sup>b</sup>
Mg II	2794.9	0.069 <sup>b</sup>
Fe II	2839.2	0.048
[Mg v]	2929.3	0.030 <sup>b</sup>
Fe II	2968.3	0.043
Fe II	2978.8	0.075
O III	3025.9	0.030
O III	3045.5	0.040
O III	3130.1	0.27
He II	3200.6	0.20

## B. INFRARED EMISSION-LINE STRENGTHS FOR AG PEGASI

Ion	Wavelength (Å)	$F/F(\text{Pa}\beta)^c$
He II	10124	1.19
He I	10830	8.25
Pa $\gamma$	10938	~0.3
Pa $\beta$	12818	1.00

<sup>a</sup>  $\text{He II } (\lambda 1640) = 115 \times 10^{-12} \text{ ergs cm}^{-2} \text{ s}^{-1}$ . Value determined from high-resolution observations of 1989 Oct 28; our saturated value  $\text{He II } (\lambda 1640) = 74.1 \times 10^{-12} \text{ ergs cm}^{-2} \text{ s}^{-1}$ .

<sup>b</sup> Saturated emission feature.

<sup>c</sup>  $F(\text{Pa}\beta) = 7.76 \times 10^{-12} \text{ ergs cm}^{-2} \text{ s}^{-1}$ .

came approximately 1 year after the 1989 October measurement for which we found a value of 115. If the flux were fractionally higher at the time of our 1989 July infrared observations, this would result in a slightly smaller reddening value than that reported in Table 9. For HM Sge and V1016 Cyg, both our measurements and those tabulated by MNSV indicate little or no variations in the He II  $\lambda 1640$  flux during the time of our observations. This is not the case for V1329 Cyg, for which the flux from 1988 April 24 is a factor of 3 larger than our value from a year later. Thus, unfortunately, there could have been substantial changes in the line fluxes in the 3 month interval that separated the infrared and ultraviolet observations.

TABLE 4

## A. ULTRAVIOLET EMISSION-LINE STRENGTHS FOR RT SERPENTIS

Ion	Wavelength (Å)	$F/F(\text{He II } \lambda 1640)^a$
N v	1236.8	0.63
C IV	1547.1	0.92
He II	1638.2	1.00
O III]	1662.8	0.27
N III]	1750.3	0.41
O III	2674.2	0.91
Fe II	2716.2	0.39
[Mg v]?	2783.8	0.39
Mg II?	2797.2	0.50
Fe II?	2816.8	0.24
O III?	3052.6	0.84
He I?	3186.3	0.83

## B. INFRARED EMISSION-LINE STRENGTHS FOR RT SERPENTIS

Ion	Wavelength (Å)	$F/F(\text{Pa}\beta)^b$
Pa $\delta$	10049	~0.3
He II	10124	0.39
He I	10830	1.50
Pa $\gamma$	10938	~0.5
He II	11626	~0.3
Pa $\beta$	12818	1.00

<sup>a</sup>  $\text{He II } \lambda 1640 = 0.19 \times 10^{-12} \text{ ergs cm}^{-2} \text{ s}^{-1}$  for 1991 Aug 2; LWR observations from 1982 Mar 2.

<sup>b</sup>  $F(\text{Pa}\beta) = 8.23 \times 10^{-13} \text{ ergs cm}^{-2} \text{ s}^{-1}$ .

Despite these two factors that can affect the He II  $\lambda 1640/\lambda 10124$  value, because of the large wavelength baseline between the two features, an error of a factor of 2 in their ratio produces an uncertainty of only 0.11 in  $E(B-V)$ . For this reason the errors in Table 9 are small. For further comparison with our values, results from other studies include, for AG Peg:  $E(B-V) = 0.05$  (Murset et al. 1991); HM Sge: 0.87 (Schmid & Schild 1990), variable from 0.45–0.70 (Bryan & Kwok 1991), 0.65 (Murset et al. 1991), V1016 Cyg: 0.31 (Ahern 1975), 0.28 (Nussbaumer & Schild 1981), 0.45 (Rudy et al. 1990), 0.53 (Schmid & Schild 1990), 0.40 (Murset et al. 1991), 0.30 (Bryan & Kwok 1991); V1329 Cyg: 0.85 (Schmid & Schild 1990), 0.60 (Murset et al. 1991).

One final remark about variability concerns the infrared data. Schmid & Schild (1990) reported Pa $\delta$ /He II  $\lambda 10124$  ratios for HM Sge, V1016 Cyg, and V1329 Cyg, and used these data to determine He/H abundance ratios for comparison with abundances obtained from optical lines. Their values are consistently larger than our ratios, for HM Sge and V1016 Cyg by approximately 60%, and for V1329 Cyg by nearly a factor of 3. We do not understand this discrepancy but note that our ratios produce He/H abundance ratios more nearly consistent with the values they derived from optical lines.

The one symbiotic nova whose reddening was not determined from the He II lines is PU Vul. Although its low-excitation spectrum does show measurable He II  $\lambda 1640$  at high resolution,  $\lambda 10124$  is too weak to determine the reddening. Fortunately, the spectrum displays strong O I  $\lambda 1304$ ,  $\lambda 8446$ , and  $\lambda 11287$ . These three features arise in a cascade from a level of neutral oxygen that is fluorescently excited by Ly $\beta$  (Bowen 1947). This process results in equal numbers of photons in each line, providing known intrinsic

TABLE 5  
A. ULTRAVIOLET EMISSION-LINE STRENGTHS FOR HM SAGITTAE

Ion	Wavelength (Å)	$F/F(\text{He II } \lambda 1640)^a$	$F/F(\text{He II } \lambda 1640)^b$
N v	1241.1	0.43	0.40
Si iv	1392.6	0.11	Blended
O iv]	1403.0	0.33	0.29
N iv]	1486.8	0.54	0.44
C iv	1550.2	1.91	2.00
[Ne iv]	1602.2	0.16	0.12
He II	1641.3	1.00	1.00
O III]	1665.7	0.22	0.19
N III]	1752.5	0.27	0.27
Si II	1816.5	0.03	...
Si III]	1894.9	0.20	0.11
C III]	1910.3	0.98	0.84
C II] + [O II]	2326.1	0.10	0.088
[Ne IV]	2420.1	0.088	0.060
[O II]	2468.1	0.050	0.066
He II	2508.9	0.031	0.032
He II	2731.4	0.083	0.096
[Mg v]	2782.7	0.39 <sup>c</sup>	0.46 <sup>c</sup>
Mg II	2792.6	0.30	0.26
Fe II	2832.5	0.083	0.084
Fe II	2850.9	0.046	0.044
Fe II?	2864.5	0.023	0.020
[Mg v]	2925.4	0.093	0.12
Fe II	2970.0	0.056	0.050
O III	3020.2	0.040	0.043
O III	3043.7	0.11	0.098
O III	3129.0	0.70	0.59
He II	3198.8	0.24	0.23

B. INFRARED EMISSION-LINE STRENGTHS FOR HM SAGITTAE

Ion	Wavelength (Å)	$F/F(\text{Pa}\beta)^d$	$F/F(\text{Pa}\beta)^e$
Pa10	9015	...	...
[S III]	9069	0.63	...
Pa9	9229	0.16	...
He II	9345	0.407	0.05
[S III], Paε	9532, 9546	2.11	2.96
Paδ	10049	0.28	0.25
He II	10124	0.82	0.95
[S II]	10287–10370	0.41	0.40
[N I]	10400	0.31	0.33
He I	10830	7.87	6.79
Paγ	10938	0.54	0.52
He II	11626	0.26	0.18
Paβ	12818	1.00	1.00

<sup>a</sup>  $\text{He II } (\lambda 1640) = 10.6 \times 10^{-12} \text{ ergs cm}^{-2} \text{ s}^{-1}$  for 1988 Mar 25.

<sup>b</sup>  $\text{He II } (\lambda 1640) = 8.64 \times 10^{-12} \text{ ergs cm}^{-2} \text{ s}^{-1}$  for 1989 Sep 7.

<sup>c</sup> Saturated emission feature.

<sup>d</sup>  $F(\text{Pa}\beta) = 1.19 \times 10^{-11} \text{ ergs cm}^{-2} \text{ s}^{-1}$  for 1988 Jul.

<sup>e</sup>  $F(\text{Pa}\beta) = 1.16 \times 10^{-11} \text{ ergs cm}^{-2} \text{ s}^{-1}$  for 1989 Jul.

line ratios from which the reddening can be determined. Continuum fluorescence of O I, which generally accompanies the Lyβ mechanism but which is weaker, corrupts these ratios slightly. Rudy et al. (1991) have described a procedure to measure the reddening from λ8446 and λ11287 using the intensity of O I λ13164, which is excited by continuum fluorescence only, to correct for the excess of λ8446 photons produced by this same mechanism. Using this procedure, as well as the one outlined by these same authors to correct for the strong telluric absorption of λ11287 (employing values of 28 km s<sup>-1</sup> for the heliocentric velocity

of PU Vul and 70 km s<sup>-1</sup> for the FWHM of O I λ11287; Bensammar et al. 1991), yields  $E(B-V) = 0.22 \pm 0.1$ .

From the ratio of λ1304 to λ8446 alone, we find  $E(B-V) \leq 0.46$ , where the upper limit results from the resonance nature of λ1304, which makes it subject to trapping and thus more susceptible to destruction by other mechanisms operating within the emission-line region (e.g., photoionization from the  $n = 2$  level of hydrogen or the metastable 2 <sup>3</sup>S level of helium, absorption by Fe<sup>+</sup>). As a further check of this method, we used it to compute the reddening of V1016, which also displays prominent O I

TABLE 6

## A. ULTRAVIOLET EMISSION-LINE STRENGTHS FOR V1016 CYGNI

Ion	Wavelength (Å)	$F/F(\text{He II } \lambda 1640)^a$	$F/F(\text{He II } \lambda 1640)^{b,c}$
N v	1238.2	1.02	0.88
O I	1303.8	0.093	0.064
Si iv	1394.5	0.25	0.22
O iv]	1400.0	0.52	0.42
N iv]	1484.7	0.32	0.26
C iv	1547.7	1.94 <sup>d</sup>	2.02 <sup>d</sup>
[Ne v]	1572.8	0.063	0.051
[Ne iv]	1599.6	0.047	0.045
He II	1639.0	1.00 <sup>d</sup>	1.00 <sup>d</sup>
O III]	1663.1	0.22	0.21
N III]	1749.1	0.13	0.11
Si II?	1815.2	0.034	0.039
Si III]	1892.0	0.17	0.17
C III]	1907.5	0.69 <sup>d</sup>	0.63 <sup>d</sup>
C II] + [O II]	2328.8	0.10	0.092
Fe II + He II	2387.0	0.018	0.024
[Ne iv]	2423.0	0.042	0.030
[O II]?	2471.6	0.020	0.016
He II + ?	2510.6	0.060 <sup>d</sup>	0.067
Fe II	2595.8	0.033	0.025
Fe II	2612.7	0.040	0.026
Fe II	2625.3	0.037	0.030
He II	2734.9	0.036 <sup>d</sup>	0.070 <sup>d</sup>
Fe II	2750.6	0.037	0.022
[Mg v]	2784.9	0.072 <sup>d</sup>	0.15 <sup>d</sup>
Mg II	2797.0	0.072 <sup>d</sup>	0.15 <sup>d</sup>
O IV + Fe II	2836.7	0.033	0.072
Fe II	2852.6	0.025	0.034
[A IV] + Fe II	2868.8	0.008	0.011
[Mg v]	2929.1	0.42 <sup>d</sup>	0.086 <sup>d</sup>
Fe II + O v?	2941.1	0.019	0.027
[Ne v]	2974.0	0.043	0.070
Fe II + N v	2980.7	0.018	...
O III	3024.5	0.034	0.030
O III	3045.6	0.055	0.061
O III	3130.9	0.25 <sup>d</sup>	0.38 <sup>d</sup>
He I	3186.2	...	0.047
He II	3200.4	0.18	0.15

## B. INFRARED EMISSION-LINE STRENGTHS FOR V1016 CYGNI

Ion	Wavelength (Å)	$F/F(\text{Pa}\beta)^e$	$F/F(\text{Pa}\beta)^f$
O I	8446	0.20	...
Pa10	9015	0.077	0.068
[S III]	9069	0.19	0.24
Pa9	9229	~0.1 <sup>g</sup>	~0.1 <sup>g</sup>
[S III], Paε	9532, 9546	0.69	0.58
Paδ	10049	0.26	0.23
He II	10124	0.56	0.50
[S II]	10287–10370	0.042	0.040
[N I]	10400	0.047	0.057
He I	10830	5.46	4.20
Paγ	10938	0.44	0.45
O I	11287	0.21	0.22
He II	11626	0.096	0.11
He II	11675	<0.03	0.022
Paβ	12818	1.00	1.00
O I	13164	<0.02	<0.03

<sup>a</sup>  $\text{He II } (\lambda 1640) = 47.0 \times 10^{-12} \text{ ergs cm}^{-2} \text{ s}^{-1}$  for 1988 Jun 19.<sup>b</sup>  $\text{He II } (\lambda 1640) = 46.0 \times 10^{-12} \text{ ergs cm}^{-2} \text{ s}^{-1}$  for 1989 Aug 12.<sup>c</sup> Although He II  $\lambda 1640$  appears saturated in both low-resolution spectra, unsaturated high-resolution *IUE* spectra from 1988 Jun 19 and 1988 Dec 16 yielded values of  $44.0 \times 10^{-12}$  and  $44.3 \times 10^{12} \text{ ergs cm}^{-2} \text{ s}^{-1}$ , respectively.<sup>d</sup> Saturated emission feature.<sup>e</sup>  $F(\text{Pa}\beta) = 1.85 \times 10^{-11} \text{ ergs cm}^{-2} \text{ s}^{-1}$  for 1988 Jul.<sup>f</sup>  $F(\text{Pa}\beta) = 1.82 \times 10^{-11} \text{ ergs cm}^{-2} \text{ s}^{-1}$  for 1989 Apr.<sup>g</sup> Affected by TiO absorption.

TABLE 7

A. ULTRAVIOLET EMISSION-LINE STRENGTHS FOR V1329 CYGNI

Ion	Wavelength (Å)	F/F(He II $\lambda$ 1640) <sup>a</sup>
N v	1242.0	0.22
Si iv	1397.2	0.039
O iv]	1403.6	0.12
N iv]	1489.3	0.16
C iv	1551.5	1.12
He II	1642.6	1.00
O III]	1666.2	0.18
N III]	1752.5	0.17
Si III]	1892.7	0.12
C III]	1911.6	0.45
[Ne iv]?	2429.7	0.066
He II?	2508.8	0.078
He II	2732.0	0.082
Fe II	2772.2	0.041
[Mg v]	2786.4	0.087
Mg II	2796.9	0.040
Fe II + O IV	2837.6	0.052
[A iv] + Fe II	2853.9	0.014
[A iv]?	2867.9	0.021
[Mg v]	2927.4	0.058
Fe II	2960.6	0.064
Fe II	2970.2	0.068
Fe II	2980.0	...
O III	3023.0	0.036
O III	3044.1	0.076
O III	3130.1	0.34
He II	3196.4	0.50

B. INFRARED EMISSION-LINE STRENGTHS FOR V1329 CYGNI

Ion	Wavelength (Å)	F/F(Pa $\beta$ ) <sup>b</sup>
O I	8446	>0.3 <sup>c</sup>
Ca II	8498	>0.07 <sup>c</sup>
Ca II	8542	>0.07 <sup>c</sup>
Ca II	8665	>0.1 <sup>c</sup>
Pa $\delta$	10049	0.19
He II	10124	0.56
He I	10830	2.15
Pa $\gamma$	10938	0.62
O I	11287	0.93
He II	11626	0.15
Pa $\beta$	12818	1.00
O I	13164	<0.08

<sup>a</sup> He II ( $\lambda$ 1640) =  $1.75 \times 10^{-12}$  ergs cm<sup>-2</sup> s<sup>-1</sup> for 1989 Apr 10.

<sup>b</sup> F(Pa $\beta$ ) =  $2.64 \times 10^{-12}$  ergs cm<sup>-2</sup> s<sup>-1</sup>.

<sup>c</sup> Affected by TiO absorption.

features. The problem for this object was that we could not obtain an accurate value for O I  $\lambda$ 13164 against the choppy stellar continuum. For  $\lambda$ 13164  $\leq$  0.02 of Pa $\beta$ ,  $E(B-V) \leq 0.4$ ; for  $\lambda$ 13164 = 0.01 of Pa $\beta$ ,  $E(B-V) = 0.25$ . The reddening from O I  $\lambda$ 8446 and  $\lambda$ 1304 alone gives  $E(B-V) = 0.25$ .

### 3.2. M Giant Classifications

Past classifications of spectral types for the giant components of the symbiotic novae have been done using optical spectra (Kenyon & Fernandez-Castro 1987, hereafter KF; Schulte-Ladbeck 1988). The former reported data from 5500 to 8600 Å and observed the six symbiotic novae presented here; the coverage of the latter extended to 9600

TABLE 8

A. ULTRAVIOLET EMISSION-LINE STRENGTHS FOR PU VULPECULAE

Ion	Wavelength (Å)	F/F(O I $\lambda$ 1302–1306) <sup>a</sup>
Si II	1265.5	0.092
O I	1305.1	1.00
[Mg v]	1327.1	0.054
C II	1338.5	0.041
Fe II	1359.8	0.24
Si IV	1395.2	0.12
O IV]	1403.2	0.26
N IV]	1487.6	0.20
?	1540.7	0.30
C IV	1548.1	0.25
He II?	1643.8	0.18
O III]?	1667.0	0.13
N III]	1750.7	0.75
Fe II	1784.8	0.26
Si II	1844.3	0.098
Al III	1856.1	0.19
Si III]	1892.3	0.74 <sup>b</sup>
C III]	1914.3	0.74 <sup>b</sup>
Fe II	2332.4	0.41
[Ne iv]?	2421.3	0.18
He II? + ?	2510.8	1.73
?	2568.9	0.13
?	2591.9	0.18
Fe II	2622.6	0.46
Al III]	2671.9	0.69
Fe II	2721.1	0.42
Fe II	2754.0	0.85
Mg II	2801.1	2.97 <sup>b</sup>
Fe II	2850.0	1.59
Fe II	2872.0	0.059
Fe II	2887.0	0.10
[Mg v]	2930.2	0.22
Fe II	2953.8	0.28
Fe II	2967.7	0.19
Fe II	2984.8	0.13
Fe II	3003.6	0.12
O III	3042.7	0.20
Ti II?	3080.7	0.25
O III	3118.6	0.054
O III	3133.7	0.10
He II	3191.0	0.52

B. INFRARED EMISSION-LINE STRENGTHS FOR PU VULPECULAE

Ion	Wavelength (Å)	F/F(Pa $\beta$ ) <sup>c</sup>
O I	8446	0.56
Ca II	8498	>0.05 <sup>d</sup>
Ca II	8542	>0.04 <sup>d</sup>
Ca II, Pa13	8662, 8665	0.060
Pa12	8750	0.040
Pa11	8863	0.043
Fe II	8927	0.06
Pa10	9015	0.08
[S III]	9069	0.058
Fe II	9123, 9132	0.07
Pa9, Fe II	9229, 9176–9205	0.36
Fe II	~9400 (blend)	0.079
[S III], Pa $\epsilon$	9532, 9546	0.17
?	~9610	0.02
Fe II	9997	0.08
Pa $\delta$	10049	0.20
He II ?	10124	0.03
Fe II	10174	0.03

TABLE 8—Continued

Ion	Wavelength (Å)	$F/F(\text{O I } \lambda\lambda 1302\text{--}1306)^a$
[S II] .....	10287–1037	<0.02
[N I] .....	10400	0.03
? .....	~10442	<0.02
Fe II .....	10490, 10501	0.085
He I, Fe II .....	10830, 10863	0.27
Pa $\gamma$ .....	10938	0.49
Fe II .....	11126	0.041
O I .....	11287	0.43
Pa $\beta$ .....	12818	1.00
O I .....	13164	0.03

<sup>a</sup> O I ( $\lambda\lambda 1302\text{--}1306$ ) =  $10.4 \times 10^{12}$  ergs  $\text{cm}^{-2}$   $\text{s}^{-1}$  for 1989 Sep 24.

<sup>b</sup> Saturated emission feature.

<sup>c</sup>  $F(\text{Pa}\beta)$  =  $6.44 \times 10^{-11}$  ergs  $\text{cm}^{-2}$   $\text{s}^{-1}$  for 1989 Jul.

<sup>d</sup> Affected by TiO absorption.

Å but included only AG Peg. KF derived spectral classifications from indices based on TiO bands at 6180 and 7100 Å, VO at 7865 Å, and Na I at 8190 Å; Schulte-Ladbeck (1988) used qualitative comparisons with field giants of known spectral type. Our classifications make use of the TiO bands at 0.85, 0.89, and 0.93  $\mu\text{m}$ ; the VO band at 1.05  $\mu\text{m}$ ; and the steam bands at 0.93  $\mu\text{m}$  and 1.14  $\mu\text{m}$ . They are complementary to the optical data in that these features are generally weaker than their optical counterparts for the same spectral type, and thus more sensitive probes at the later spectral types. Examples include the VO feature and steam bands, which do not appear until spectral type M5 (Spinrad & Wing 1969; Hinkle & Barnes 1979). These features are advantageous in classifying the later objects where many of the optical bands are saturated. Our spectral classifications are listed in Table 10, along with the values reported by KF. Brief explanations of the rationale for each classification follow.

AG Peg has the bluest stellar continuum of any symbiotic novae we observed. A blackbody curve fitted to the spectrum yields a color temperature of  $\sim 3000$  K. The absence of VO at 1.05  $\mu\text{m}$  indicates a spectral type earlier than M5. The absence of the broad TiO absorption 0.93  $\mu\text{m}$  indicates a spectral type earlier than M4, and this limit is the best constraint we can place on the spectral type. At shorter

TABLE 10  
SPECTRAL CLASSIFICATIONS FOR THE RED GIANTS IN  
SYMBIOTIC NOVAE

Object	Spectral Class (This Work) <sup>a</sup>	Spectral Class (KF <sup>b</sup> )
AG Peg .....	<M4	M3
RT Ser .....	M5.5	M5.5
HM Sge (1988) .....	M5	>M4
HM Sge (1989) .....	M7	...
V1016 Cyg (1988) .....	M6.5	>M4
V1016 Cyg (1989) .....	M6	...
V1329 Cyg .....	M5.5	>M4
Pu Vul .....	~M4	M4–M5

<sup>a</sup> Uncertainties are approximately  $\pm 0.5$  of a spectral class.

<sup>b</sup> Kenyon & Fernandez-Castro (1987).

wavelengths, however, TiO absorptions are clearly present (KF). These authors classify the giant as  $M3 \pm 0.4$  III, a value we will adopt to estimate the distance.

For RT Ser the 1.05  $\mu\text{m}$  VO band and the TiO absorption features form the basis for the classification. The weak but detectable presence of the former plus the depth of the latter indicate a spectral type of M5.5 with a possible range of about  $\pm 0.5$  of a spectral class.

HM Sge is one of the two known Mira variables in our sample of symbiotic novae. Its large fluctuations are clearly apparent in Figure 3c. The absence of measurable VO and the weakness of the TiO trough at 0.93  $\mu\text{m}$  leads to an approximate classification of M5 from the 1988 data. In contrast, the deep, broad VO absorption in the 1989 spectrum indicates a much later spectral class of M7 for the HM Sge Mira component at this date.

V1016 is the second Mira variable in our sample. Although the change in brightness and spectral type were less pronounced than HM Sge, its variations are apparent in Figure 4c. On the basis of the slightly deeper steam band between 1.1 and 1.2  $\mu\text{m}$  at the earlier epoch, we classify the giant as M6.5 in 1988 and M6 in 1989.

V1329 Cyg displays a near-infrared stellar continuum that is virtually identical to that of RT Ser. From the same features we also classify it as M5.5, somewhat later than the value of M4 suggested by Schmid & Schild (1990).

The continuum of PU Vul is blurred by the large number of emission lines. Although partially filled by these features,

TABLE 9

HE II RATIOS AND REDDENING VALUES FOR SYMBIOTIC NOVAE

Object	He II ( $\lambda 1604/\lambda 10124$ ) (This Work)	$N_e^a$ ( $\text{cm}^{-3}$ )	$T_e^a$ ( $\times 10^4$ )	$E(B-V)^b$ (This Work)	$E(B-V)$ (MN <sup>c</sup> )
AG Peg .....	12.5	$1.0 \times 10^9$	1.2	0.14	0.05
RT Ser .....	0.60	$1.0 \times 10^9$	1.2	$0.64 \pm 0.1$	0.5
HM Sge (1988) .....	1.09	$1.0 \times 10^6$	2.0	0.53	0.65
HM Sge (1989) .....	0.79	$1.9 \times 10^6$	2.0	0.58	...
V1016 Cyg(1988) .....	5.38	$1.0 \times 10^6$	2.0	0.28	0.40
V1016 Cyg(1989) .....	5.04	$1.0 \times 10^6$	2.0	0.29	...
V1329 Cyg .....	1.19	$1.0 \times 10^9$	2.0	0.53	0.60
Pu Vul .....	...	$>1.0 \times 10^{10}$	...	0.22 <sup>d</sup>	0.40

<sup>a</sup> References for densities and temperatures: AG Peg: Murset et al. (1991), Nussbaumer et al. (1988); RT Ser: Nussbaumer et al. (1988); HM Sge, V1016 Cyg, V1329 Cyg: Schmid & Schild (1990); PU Vul: Vogel & Nussbaumer (1992).

<sup>b</sup> Errors are  $\pm 0.04$  unless otherwise noted.

<sup>c</sup> Murset & Nussbaumer (1994).

<sup>d</sup> For PU Vul,  $E(B-V) = 0.22 \pm 0.1$  was derived from the O I lines (see text).

the TiO absorptions at 0.85, 0.89, and 0.93  $\mu\text{m}$  are present, though not at the strength of their counterparts in V1329 Cyg. Taken together with the absence of VO at 1.05  $\mu\text{m}$ , this suggests a classification of M4 to M5. This is the same as found by KF. The later spectral types found by Schmid (1990) and Schild, Boyle, & Schmid (1992) are incompatible with the absence of the VO band.

### 3.3. Distance Estimate

The distance to each system was determined from the method of spectroscopic parallaxes. This makes use of our near-IR measurement of the apparent brightness, the extinction value from Table 9, and the absolute magnitude of the giant component at 1.25  $\mu\text{m}$  as derived from the spectral type. The apparent  $J$  magnitudes were obtained by convolving the near-IR spectrum with the filter profile of the standard  $J$  filter. They are presented in Table 11 together with magnitudes from the previous photometric studies of Allen (1982), Kenyon (1988), and Munari et al. (1992). The total extinction in  $J$  band,  $A_J = 0.87E(B-V)$ , was taken from Savage & Mathis (1979), and the absolute magnitude  $M_J$  for each giant was computed from the intrinsic color difference  $V - J$  (Koornneef 1983) and the absolute visual magnitude  $M_V$  (Thé et al. 1990) of the corresponding spectral type.

The largest sources of error in this process are the uncertainty in our spectral classification, and the spread in the expression relating absolute magnitude to spectral type. We estimate the error in spectral class to be about  $\pm 0.5$  of a class, similar to the values quoted in other studies (e.g., KF) implying an error of no more than 0.25 mag in  $M_J$  for the M giants. The spread in relationship between  $M_V$  and spectral

type, as estimated from inspection of the different data sets compiled by Thé et al. (1990), is comparable. Allowing for some uncertainty in the reddening and in the  $V - J$  color still yields a total formal error less than 0.5 mag and a corresponding uncertainty in the distance smaller than 25%. However, there is a possibility that the intrinsic luminosities of the Mira variables are greater than the values inferred from their spectral types, a topic that will be discussed in the next section.

## 4. DISCUSSION

The physical parameters of the symbiotic systems that we have derived from the IR and UV spectrophotometry, namely the reddening, spectral classification of the giant component, and distance, are presented in Tables 9, 10 and 12. Values for all these parameters exist in the earlier literature and in only a few instances do our results differ significantly from those; in most cases they simply confirm or refine the previous values. Nevertheless, it is worthwhile considering the discrepancies and possible reasons for them.

With regard to the reddening values, the only objects for which there is a discrepancy with past studies are RT Ser and PU Vul. MN derived the reddening for the former from the ratio of the He II lines  $\lambda 4686$  and  $\lambda 5411$  measured by Fried (1990b). Although the value of  $E(B-V) = 0.5$  is close to our value of 0.6, the Balmer decrement taken from Fried's spectroscopy suggests the significantly larger value  $E(B-V) = 1.0 \pm 0.1$ . While use of the hydrogen line ratios as a reddening metric is suspect since the emission-line region clearly does not satisfy Case B conditions (as noted by Fried himself), the large disparity between reddening

TABLE 11  
J MAGNITUDES FOR SYMBIOTIC NOVAE

Object	This Work <sup>a</sup>	Munari et al. (1992)	Kenyon (1988)	Allen (1982)
AG Peg.....	5.01	5.06	5.03–5.13	5.12
RT Ser.....	8.42	8.36	8.44	8.53
HM Sge (1988).....	8.37	7.22–7.59	6.63–8.96	7.4–8.2
HM Sge (1989).....	6.95	7.22–7.59	6.63–8.96	7.4–8.2
V1016 Cyg (1988).....	7.67	6.63–7.88	7.23–7.93	...
V1016 Cyg (1989).....	8.20	6.63–7.88	7.23–7.93	...
V1329 Cyg.....	8.21	8.25	8.33–9.04	8.53
Pu Vul.....	7.42	6.87	7.28	...

<sup>a</sup> Errors are  $\pm 0.1$  mag.

TABLE 12  
SPECTRAL TYPE, ABSOLUTE MAGNITUDES, AND DERIVED DISTANCES

Object	Spectral Type	$M_J$	Distance (kpc) (This Work)	Distance (kpc) (MN <sup>a</sup> )
AG Peg.....	M3	–4.61	0.82	0.65
RT Ser.....	M5.5	–5.92	5.8	9
HM Sge (1988).....	M5	–5.65	5.2	2.9 <sup>b</sup>
HM Sge (1989).....	M7	–6.38	3.7	...
V1016 Cyg (1988).....	M6.5	–6.29	5.6	3.9 <sup>b</sup>
V1016 Cyg (1989).....	M6	–6.19	6.8	...
V1329 Cyg.....	M5.5	–5.92	5.5	3.4
Pu Vul.....	M4.5	–5.38	3.2	1.8

<sup>a</sup> Murset & Nussbaumer (1994).

<sup>b</sup> From period/luminosity relationship for Mira variables (Feast et al. 1989).

value derived from the Balmer decrement and that indicated by the He II lines suggests that the reddening for this object is still somewhat uncertain. For PU Vul, our value of 0.22 is smaller than the value of  $E(B - V) = 0.4 - 0.5$  reported by Kenyon (1986) and Vogel & Nussbaumer (1992). The method and problems in determining the reddening have been discussed above and the O I lines, which we used to measure the reddening in PU Vul, do not provide as accurate a method as the well separated UV and IR He II features.

There have not been nearly as many classifications of the M giant components as there have been determinations of the reddening. The largest disparities between our values and those present in the literature are for the latest spectral types where the optical determinations are very uncertain. The very late types we have assigned to V1016 Cyg and HM Sge are entirely consistent with their Mira natures.

Only our distances, which are derived from the other quantities, depart consistently from past values. (The exception is AG Peg.) The large distance for RT Ser (9 kpc) reported by MN was drawn originally from the work of Allen (1980b). While the photometry on which this estimate was based is similar to that of later epochs, a later spectral type (M6) was assumed and no correction for reddening included; both factors which increased the derived distance. Using his  $K$  magnitude together with our spectral type and reddening value, yields 6.3 kpc, much closer to our value of 5.8. With regard to V1329 Cyg, MN employed a much earlier spectral type (M4) than is consistent with the VO feature seen in our data. This accounts for the bulk of the differences in the distances of Table 12—a small amount is also due to the older references they used for  $M_V$  versus spectral class, and  $V - K$  color versus spectral class (Schmidt-Kaler 1982; Johnson 1966, respectively). Using their photometry and reddening together with our spectral type and the Thé et al. (1990) and Koornneef (1983) values for absolute magnitude and color as a function of spectral class results in a distance of 5.9 kpc versus the 5.5 found by us. The distance of 1.8 kpc for PU Vul was derived by Vogel & Nussbaumer (1992) from eclipse considerations; we

cannot reconcile this with our value of 3.2 but we note that the distance implied by the  $K$  magnitude of Munari et al. (1992) and the spectral type and reddening of MN is 3.1 kpc.

In the case of V1016 Cyg and HM Sge, MN have used the period/luminosity relations of Feast et al. (1989) for Mira variables to derive luminosities from the known periods ( $\sim 450$  and 540 days, respectively; Whitelock 1988). These give higher intrinsic luminosities than the values inferred from the spectral type and actually increase the derived distance. (If distances are computed on the basis of the absolute  $J$  magnitude and period relation given by these same authors, the distances for HM Sge and V1016 Cyg, respectively, are less than 7.1 kpc and less than 8.6 kpc, where the “less than” results from not observing either object at maximum brightness.) We believe the reason for the discrepancy between our distances for these two objects and the much smaller values of MN is due to the reddening estimates. Whitelock (1988) noted that the Mira components produce dust in their outer atmospheres that can give rise to a local reddening much greater than that of the emission-line region. In fact, Whitelock (1988) quotes extinction values of  $A_K = 1.2$  and 0.9 for HM Sge and V1016 Cyg, respectively [i.e.,  $E(B - V) = 3.2$  and 2.4], and these values are reflected in the distances reported by MN. Rudy et al. (1990) have argued against such a high value in V1016 Cyg based on the shape of the near-infrared stellar continuum; consequently we use only the extinction value deduced from the emission lines in estimating the distance. An identical analysis for HM Sge does not indicate any significant additional reddening for the giant component at the times of our observations.

We are grateful to K. Baker, J. Burrous, W. Earthman, and J. Morey, the telescope operators at Lick Observatory, for their help in acquiring these observations. H. Schmid and S. Shore provided a number of helpful comments and references. This work was supported by the Aerospace Sponsored Research program. R. C. P. acknowledges support from NASA.

#### REFERENCES

- Ahern, F. J. 1975, *ApJ*, 197, 639  
 Allen, D. A. 1980a, *MNRAS*, 190, 75  
 ———, 1980b, *MNRAS*, 192, 521  
 ———, 1982, *MNRAS*, 192, 521  
 Ananth, A. G., & Leahy, D. A. 1993, *J. Ap. Astr.*, 14, 37  
 Andriolat, Y. 1982, in *The Nature of Symbiotic Stars*, ed. M. Friedjung & R. Viotti (Dordrecht: Reidel), 47  
 Andriolat, Y., & Houziaux, L. 1994, *MNRAS*, 271, 875  
 Baratta, G. B., Neto, A. D., Rossi, C., & Viotti, R. 1991, *A&A*, 251, 75  
 Bensammar, S., Friedjung, M., Chauville, J., & Letourneur, N. 1991, *A&A*, 245, 575  
 Bowen, I. S. 1947, *PASP*, 59, 196  
 Bragaglia, A., Duerbeck, H. W., Munari, U., & Zwitter, T. 1995, *A&A*, 297, 759  
 Bryan, G. L., & Kwok, S. 1991, *ApJ*, 368, 252  
 Doschek, G. A., & Feibelman, W. A. 1993, *ApJS*, 87, 331  
 Feast, M. W., Glass, I. S., Whitelock, P. A., & Catchpole, R. M. 1989, *MNRAS*, 41, 375  
 Fried, J. W. 1990a, *A&A*, 81, 182  
 ———, 1990b, *A&AS*, 83, 301  
 Grandi, S. 1980, *ApJ*, 238, 10  
 Hamann, F., DePoy, D. L., Johansson, S., & Elias, J. 1994, *ApJ*, 422, 626  
 Hayes, D. S., & Latham, D. W. 1975, *ApJ*, 197, 593  
 Hinkle, K. H., & Barnes, T. G. 1979, *ApJ*, 227, 923  
 Hric, C., Chochol, D., & Komzik, R. 1993, *Ap&SS*, 201, 107  
 Hummer, D. G., & Storey, P. J. 1987, *MNRAS*, 224, 26  
 Ivison, R. J., & Seaquist, E. R. 1995, *MNRAS*, 272, 878  
 Johansson, S. 1990, in *ASP Conf. Ser. 9, Cool Stars, Stellar Systems, and the Sun*, ed. G. Wallerstein (San Francisco: ASP), 307  
 Johansson, S., & Jordan, C. 1984, *MNRAS*, 210, 239  
 Johnson, H. L. 1966, *ARA&A*, 4, 193  
 Kelly, D. M., & Latter, W. B. 1995, *AJ*, 109, 1320  
 Kenyon, S. J. 1986, *AJ*, 91, 563  
 ———, 1988, *AJ*, 96, 337  
 Kenyon, S. J., & Fernandez-Castro, T. 1987, *AJ*, 93, 938 (KF)  
 Klein, A., Bruch, A., & Luthardt, R. 1994, *A&AS*, 104, 99  
 Koornneef, J. 1983, *A&A*, 128, 84  
 Kurucz, R. L. 1988, Commission 14 on Atomic and Molecular Spectroscopy, *Trans. IAU*, Vol. XXB, ed. M. McNally (Dordrecht: Kluwer), 168  
 ———, 1991, *Precision Astronomy: Astrophysics of the Galaxy*, ed. A. G. Davis Philip, A. R. Upgren, & K. A. Janes (Schenectady: Davis)  
 Meier, S. R., Kafatos, M., Fahey, R. P., & Michalitsianos, A. G. 1994, *ApJS*, 94, 83  
 Mikolajewska, J., & Kenyon, S. J. 1996, *AJ*, 112, 1659  
 Munari, B. F., et al. 1992, *A&AS*, 93, 383  
 Murset, U., & Nussbaumer, H. 1994, *A&A*, 282, 586 (MN)  
 Murset, U., Nussbaumer, H., Schmid, H., & Vogel, M. 1991, *A&A*, 248, 458  
 Nussbaumer, H., & Schild, H. 1981, *A&A*, 101, 118  
 Nussbaumer, H., & Schild, H. M., Schmid, H. M., & Vogel, M. 1988, *A&A*, 198, 79  
 Penston, M. V., et al. 1983, *MNRAS*, 202, 833  
 Rudy, R. J., Cohen, R. D., Rossano, G. S., & Puetter, R. C. 1990, *ApJ*, 362, 346  
 Rudy, R. J., Erwin, P., Rossano, G. S., & Puetter, R. C. 1991, *ApJ*, 383, 344  
 ———, 1992, *ApJ*, 398, 278  
 Savage, B. D., & Mathis, J. S. 1979, *ARA&A*, 17, 73  
 Schild, H., Boyle, S. J., & Schmid, H. M. 1992, *MNRAS*, 258, 95  
 Schild, H., & Schmid, H. M. 1997, *A&A*, 324, 606  
 Schmid, H. M. 1990, Ph.D. thesis, ETH Zurich  
 Schmid, H. M., & Schild, H. 1990, *MNRAS*, 246, 84

- Schmidt-Kaler, T. 1982, in Landolt-Borstein, New Ser., Group 6, Vol. 2, Astronomy and Astrophysics (Berlin: Springer), 449
- Schulte-Ladbeck, R. E. 1988, A&A, 189, 97
- Shore, S. N., & Aufdenberger, J. P. 1993, ApJ, 416, 355
- Slovak, M. H., & Lambert, D. L. 1988, in The Symbiotic Phenomenon, ed J. Mikolajewska, M. Friedjung, S. J. Kenyon, & R. Viotti (Dordrecht: Kluwer), 265
- Spinrad, H., & Wing, R. F. 1969, ARA&A, 7, 249
- Thé, P. S., Thomas, D., Christensen, C. G., & Westerlund, B. E. 1990, PASP, 102, 565
- Viotti, R. 1988, in The Symbiotic Phenomenon, ed. J. Mikolajewska, M. Friedjung, S. J. Kenyon, & R. Viotti (Dordrecht: Kluwer), 269
- Vogel, M., & Nussbaumer, H. 1992, A&A, 259, 525
- Whitelock, P. 1988, in The Symbiotic Phenomenon, ed. J. Mikolajewska, M. Friedjung, S. J. Kenyon, & R. Viotti (Dordrecht: Kluwer), 47